Olena Mezhenska

INVESTIGATION OF THE *DP → DP* AND *DP → PPN* REACTIONS AT INTERMEDIATE ENERGIES AT NUCLOTRON

Workshop EJČF , Jun 11 – 18, 2022

Outline

- ✓ Introduction:
  - motivation;
  - polarization observables in elastic scattering;
  - dp-breakup kinematics.
- ✓ Data analysis of the results on the measurements of $\boldsymbol{A_y}$, $\boldsymbol{A_{yy}}$, $\boldsymbol{A_{xx}}$ in *dp* – elastic scattering at the energy of 800 MeV:
  - selection of the *dp*-elastic scattering events;
  - signal selection by CH_2 and ^{12}C data subtraction;
  - results.
- ✓ Data analysis of the results in *dp* – breakup at the energies below 500 MeV:
  - Amplitude correction;
  - energy calibration;
  - calculation of the efficiency of the detectors;
  - S – curve;
- ✓ Conclusions.

Motivation

Understanding the nature of the nuclear force is one of the most important questions in nuclear physics.
The detailed knowledge of the nuclear forces provides description of the nuclear properties and their reactions.

Two Nucleon Force (2NF)

1935 Yukawa's meson theory (2NF)

Theory :
- ✓ One Pion Exchange Model
- ✓ One Boson Exchange Model

1990's Realistic Modern NN Force CD Bonn, AV18, Nijmegen I,II,93

Three Nucleon Force (3NF)

1957 Fujita-Miyazawa 3NF

2π-exchange 3NF :
- Main Ingredients :

Δ - isobar excitations in the intermediate

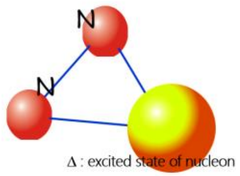

Tucson-Melbourne (TM) , Urbana IX, etc…

2NF and 3NF effects can be studied using polarization observables in *dp−> dp*. The dp elastic scattering reaction has been investigated at the energy of 800MeV covered the angular region of 60°–135° in cms.

The dp breakup reaction has been investigated at the angles of 19 – 54 degrees in the laboratory frame at the energy of 300 - 500 MeV in a various detector configurations, in which the sensitivity to the three nucleon correlations and relativistic effects are assumed.

Motivation

Experiments

✓ **KVI:**

- differential cross-section and analyzing power measurements of the *p* + *d*, *d* + *p*, and *d* + *d* reactions at the energy rage of 90 - 250 MeV at $30^{\circ} < \theta_{c.m.} < 150^{\circ}$;
- differential cross section and analyzing power of the dp-breakup.

✓ **RIKEN:**

- differential cross section and polarization observables of the p + d elastic scattering at the energy 140, 200, 250, 280 MeV at $10^{\circ} < \theta_{c.m.} < 180^{\circ}$;

✓ **RNCP**

- differential cross section and polarization observables of the p + d elastic scattering at the energy of 250 MeV at $10^{\circ} < \theta_{c.m.} < 165^{\circ}$;

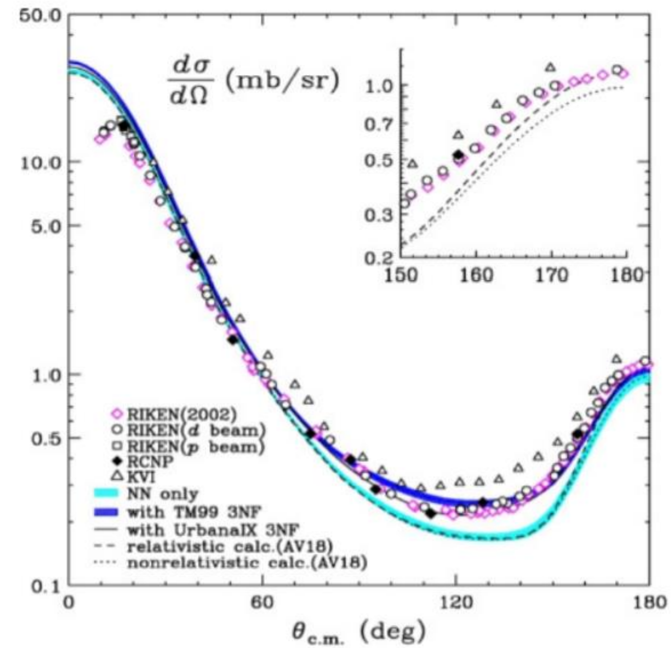

Fig.1: The differential cross section in pd-elastic scattering process at the energy of 135 MeV/nucleon.
The experimental data are given by symbols.
The curves represent various theoretical models.
The insertion shows a zoom of the backward angle part.

K. Sekiguchi et al. Phys. Rev. Lett. 95, 162301 (2005).

Motivation

3NF, dp - breakup

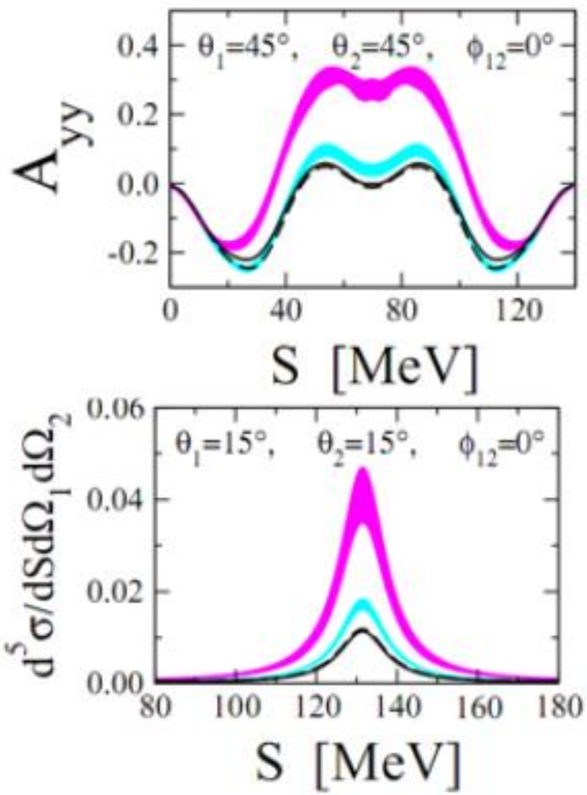

Fig.2: Tensor analyzing power A_{yy} and differential cross section at 200 MeV.

The light blue band contains theoretical predictions on CD-Bonn, AV18, Nijm I, II and Nijm 93;

The darker magenta band represents predictions NN + 3NF;

The solid line is for AV18+Urbana IX and the dashed line for CD Bonn+TM.

Θ_1 – polar angle of the 1-st proton.
Θ_2 – polar angle of the 2-nd proton.
S – arc length along the kinematical curve.
Φ_{12} – azimuth angle with respect to the horizontal plane.

One can see that the inclusion of 3NF have great impact on the values of the analyzing power and cross section.

Motivation

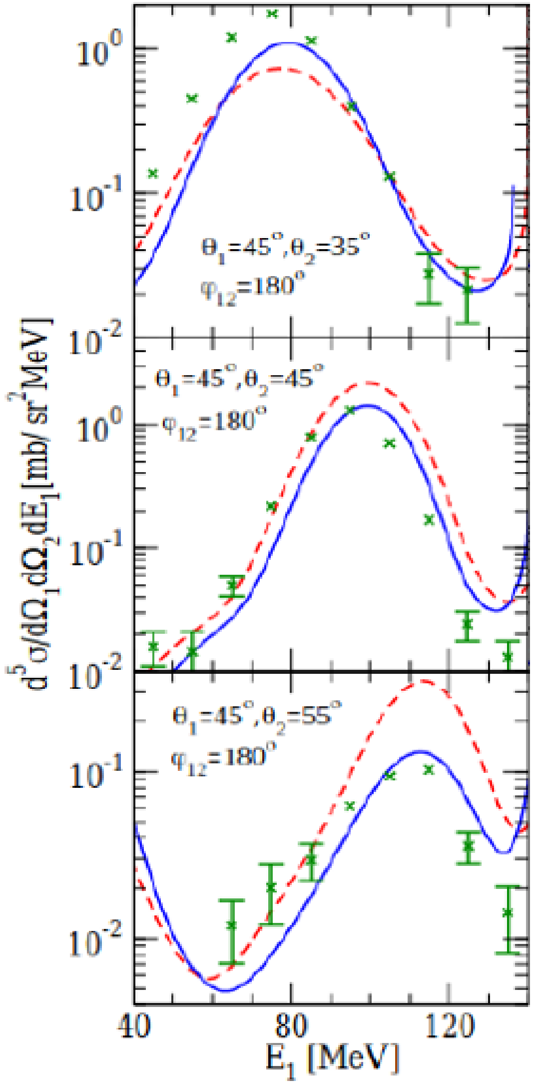

In some regions of phase space, besides the 3N force, the relativistic effect can be observed.

- ✓ The red curve is the nonrelativistic prediction;
- ✓ the blue one is the corresponding relativistic results;
- ✓ one arm is fixed, second arm scans angular range.

Important contribution comes from relativistic effects.

Fig.3: The cross section of the dp-brekup reaction at 200 MeV.

H. Witala, Few Body Syst. (2011) 49, 61.

Polarization observables in elastic scattering

S = 1 particles

Cross section

$$\sigma(\theta,\phi) = \sigma_0(\theta,\phi)[1 + \frac{3}{2}p_y A_y(\theta) + \frac{2}{3}p_{xz}A_{xz}(\theta) + \frac{1}{3}p_{xx}A_{xx}(\theta) + \frac{1}{3}p_{yy}A_{yy}(\theta) + \frac{1}{3}p_{zz}A_{zz}(\theta)].$$

σ_0 - the cross section of the scattering reaction for unpolarized beam,
p_y - the deuteron beam vector polarization,
p_{ij} - the tensor polarization
A_y - the vector analyzing power,
A_{ij} - tensor analyzing powers.

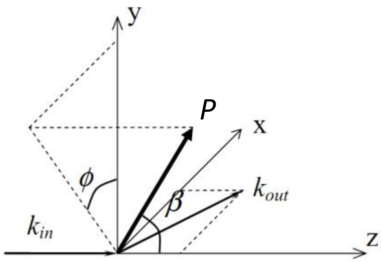

$$p_y = P_z,$$
$$p_{yy} = P_{zz},$$
$$p_{xx} = p_{zz} = -\frac{1}{2}P_{zz}$$
$$p_x = p_z = p_{xy} = p_{yz} = p_{xz} = 0.$$

$$P_z = N_+ - N_-,$$
$$P_{zz} = N_+ + N_- - 2N_0 = 1 - 3N_0$$

N_+, N_0, N_- — the relative population of particles with the orientation of the magnetic moment + 1, 0, −1

The relations between the normalized outputs for to the left (along X-axis), to the right (against X-axis), up (along Y- axis), d (against Y –axis):

$$L = 1 + \frac{3}{2}P_z A_y + \frac{1}{2}P_{zz}A_{yy},$$
$$R = 1 - \frac{3}{2}P_z A_y + \frac{1}{2}P_{zz}A_{yy},$$
$$U = 1 + \frac{1}{2}P_{zz}A_{xx},$$
$$D = 1 + \frac{1}{2}P_{zz}A_{xx},$$

Analyzing powers:

$$A_y = \frac{1}{3}\frac{L-R}{P_z},$$
$$A_{yy} = \frac{L+R-2}{P_{zz}},$$
$$A_{xx} = \frac{2}{P_{zz}}(U(D) - 1).$$

Breakup reaction

Kinematics

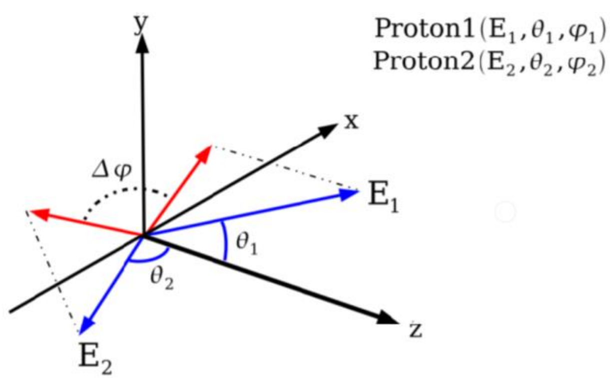

The final state particles can be determined using

$$(E_1, \theta_1, \phi_1)_{p_1}, (E_2, \theta_2, \phi_2)_{p_2}, (E_3, \theta_3, \phi_3)_{n};$$

\+ four momentum conservation law:

$$Q + 2[(E_1 + E_2)(E_p + m_d) - \sqrt{(E_1^2 - m_1^2)(E_p^2 - m_p^2)}cos\theta_1 - \sqrt{(E_2^2 - m_2^2)(E_p^2 - m_p^2)}cos\theta_2 + \sqrt{(E_1^2 - m_1^2)(E_2^2 - m_2^2)}cos\theta_{12} - E_p m_d - E_1 E_2] = 0,$$

$$Q = m_3^2 - m_1^2 - m_2^2 - m_d^2 - m_p^2$$

The dependence of E_2 on E_1 is the S - curve

The S-curve contains all the kinematically allowed combinations of E_1 and E_2

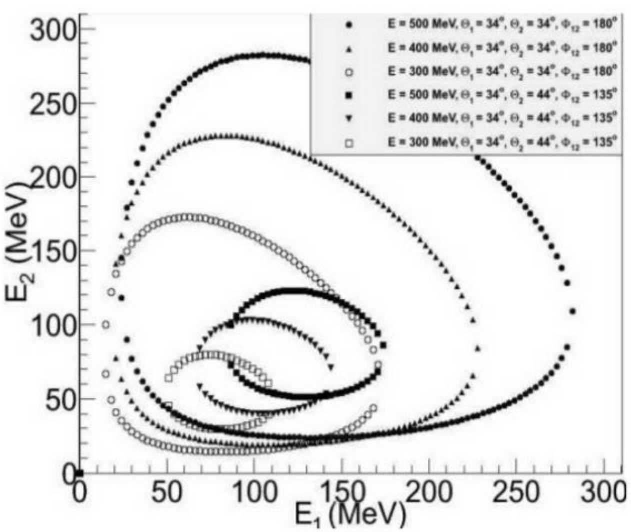

Fig. 4: The energy of the second proton as a function of the energy of the first proton is represented as the S-curve.

DSS

The experimental data were obtained at the ITS at Nuclotron **in the framework of the DSS project**.

The purpose of the DSS experimental program is to obtain the information about 2NF and 3NF from two processes

- ✓ dp-elastic scattering at the energies between 300 - 2000 MeV
- ✓ dp-breakup with registration of two protons at deuteron energies of 300 - 500 MeV

measurement of

- ➢ cross-section
- ➢ vector Ay analyzing power
- ➢ tensor Ayy & Axx analyzing powers

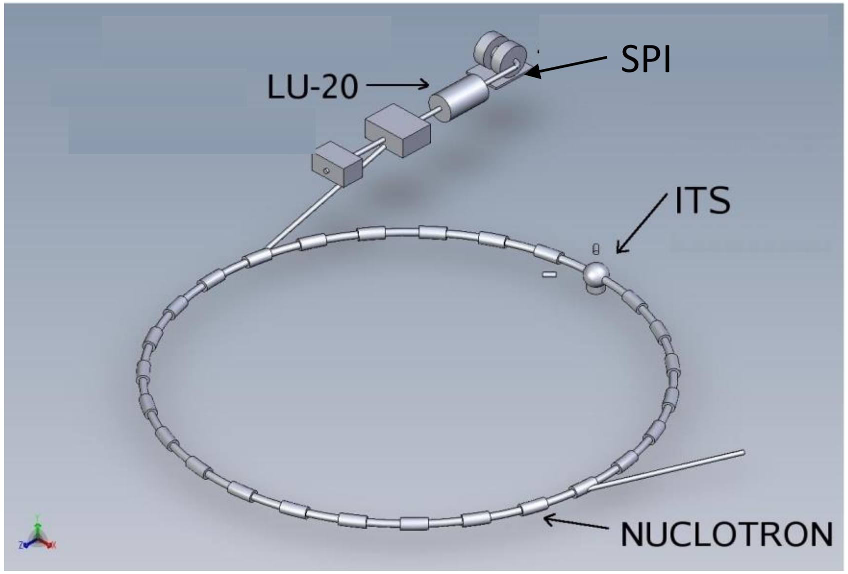

Fig.5: Nuclotron accelerator complex.

Fig.6: The view of the Internal Target Station.

dp – elastic scattering

- Experimental setup;
- selection of the dp-elastic scattering events;
- signal selection by CH_2 and ^{12}C data subtraction;
- angular dependence of the analyzing powers.

Particle detection system for dp-elastic scattering

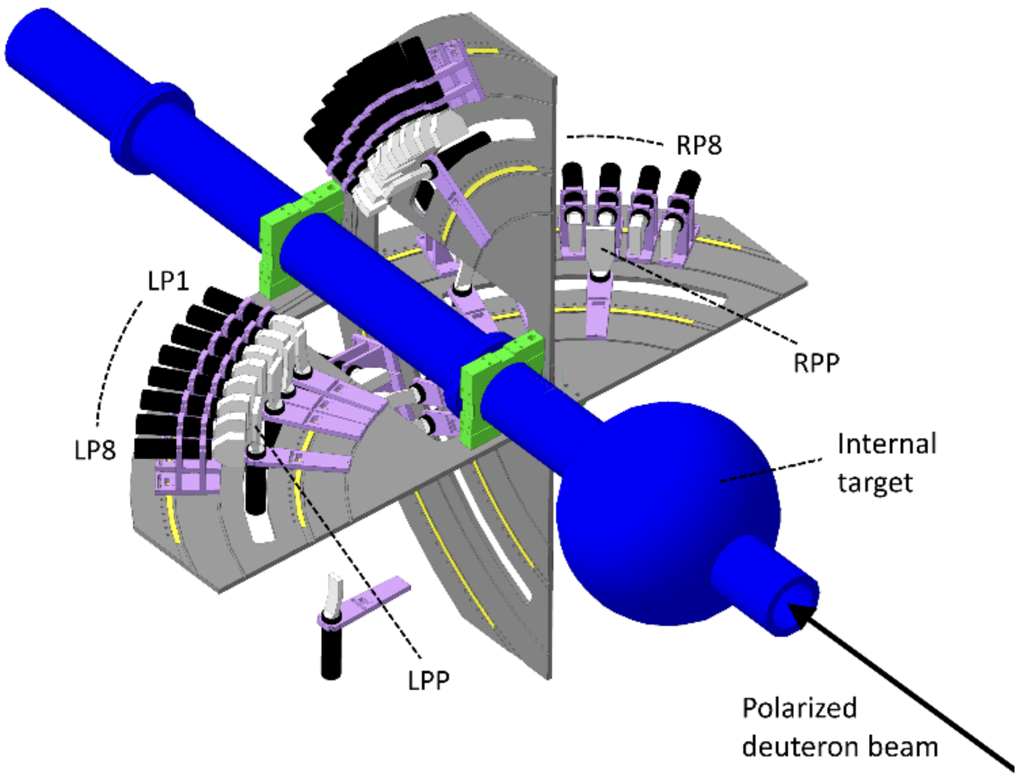

Fig.7: Arrangement of the detectors for dp-elastic scattering investigation installed downstream the ITS at Nuclotron.

- Deuterons and protons in coincidences using scintillation counters ;
- two runs of data at "even" angles (60° , 71.5° , 80° , 91° , 100° , 110° , 120.5° , 131°) and one at "odd angles" (65° , 75° , 84° , 95° , 105° , 115° , 124.5°)
- internal beam and thin CH_2 target (C for background estimation) ;
- polarization measurement at 270 MeV;
- analyzing powers measurement at 800 MeV;
- the data were taken for three spin mode of SPI: (p_z,p_{zz}) = (0,0), (1/3,1) and (1/3,-1).

Events selection

The interaction point is shifted relative to the center of the ion tube.

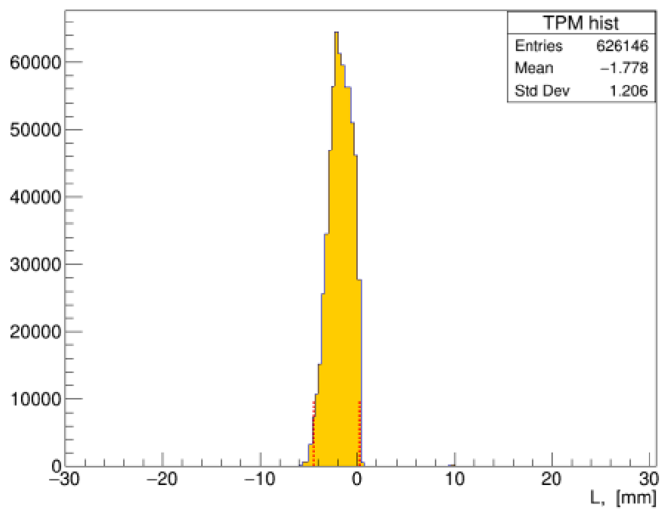

Fig.8: The distribution of the position of the interaction point of beam with the target.

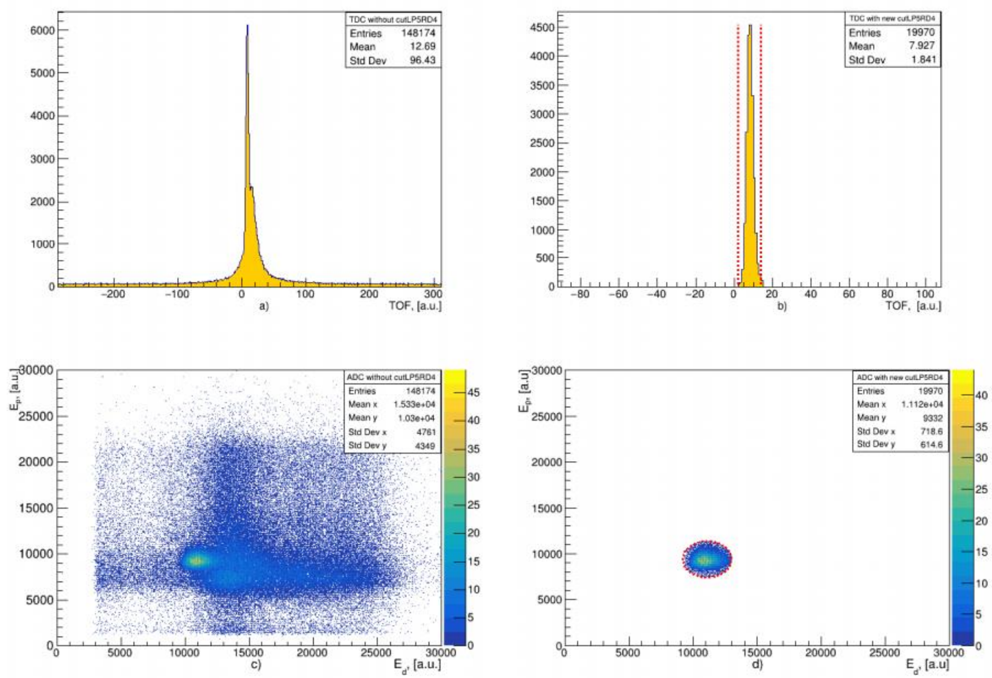

Fig.9: Selection of the dp-elastic events by the time-of-flight difference (a, b) and the correlation of the energy losses signals (c, d) for a pair signal for a pair of deuteron and proton detector at 105° in c.m.s.

The red lines represents a graphical cut for the selection of the elastic scattering event

The graphical cuts are applied to all pairs of the coincidence detectors for each runs.

$CH_2 - C_{12}$ subtraction

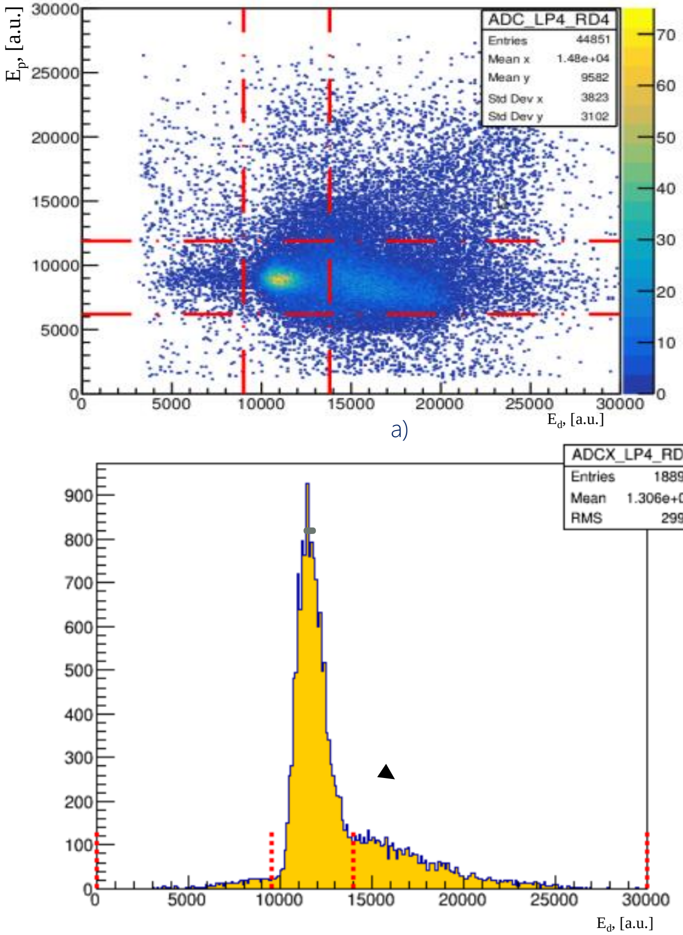

Fig.10: The energy losses signal (a) and projection (b).

The number of useful events of dp interactions

$$N_{dp} = N_{CH_2} - kN_C$$

The normalization coefficient *k* was found by using the least squares method:

$$f(k) = \{\sum_i (N_i^{CH_2} - kN_i^C)\}^2$$

← *should take the smallest value*

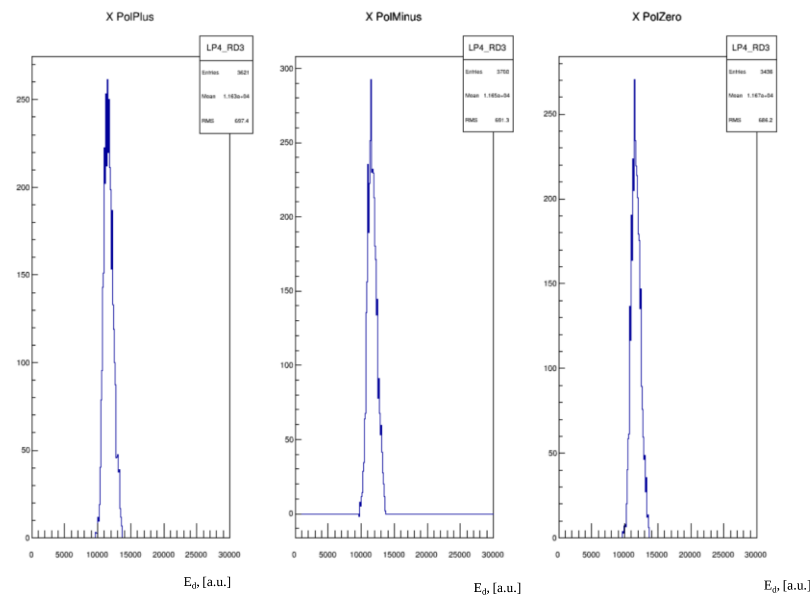

Fig.11: Projection of the energy losses signal in the pair of the detectors at X-axis after $CH_2 - C_{12}$ procedure.

Angular dependence of the analyzing powers

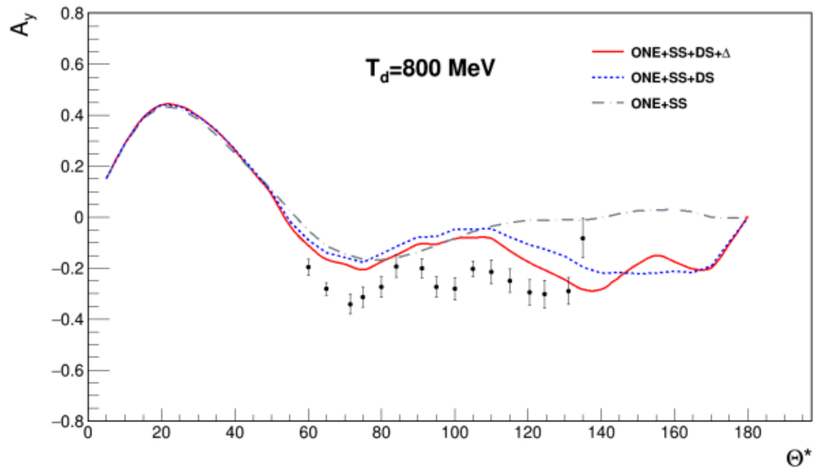

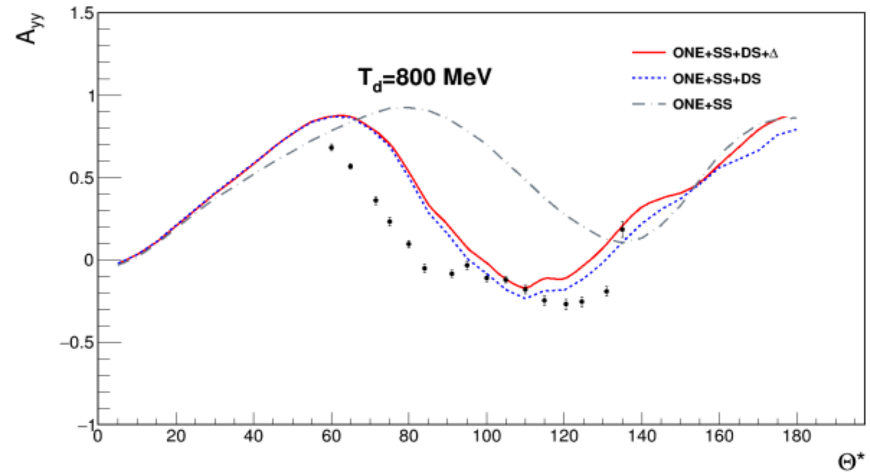

Fig.12: Vector (A_y) and tensor (A_{yy}, A_{xx}) analyzing powers of the dp-elastic scattering at the energy of 800 MeV as a function of scattering angle.

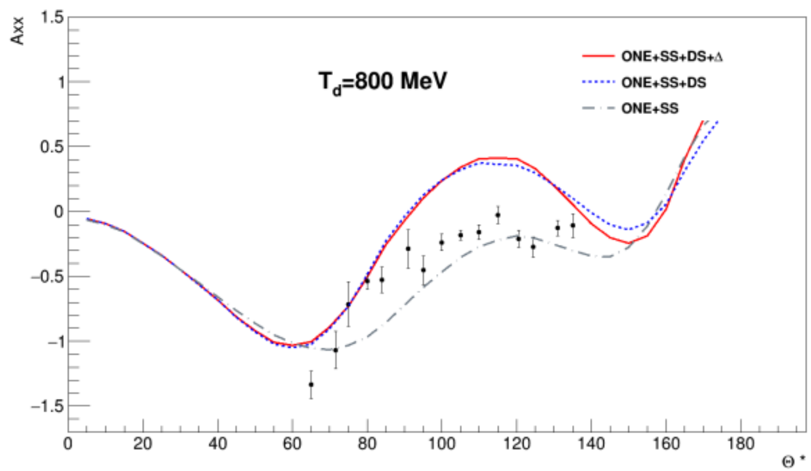

(— - **N.B.Ladygina, Eur.Phys.J, A52 (2016) 199,**

– –, — - **N.B.Ladygina, Eur.Phys.J, A42 (2009) 91**)

dp – breakup

- Particle detection system;

- Calibration measurement at the 300, 400, 500 MeV at kinematics which satisfies pp - quasi elastic reaction under **90**° in the cms:

  1) amplitude corrections using LED amplitude information;
  2) positional dependence correction of the PMT's amplitude placed of thin scintillator;
  3) calculation of the calibration coefficients .

- The dp - breakup experiment at 300 MeV in the space star configuration:

  1) Calculation of the detector efficiency;
  2) Projection of the experimental data onto S – curve.

Particle detection system for dp - breakup

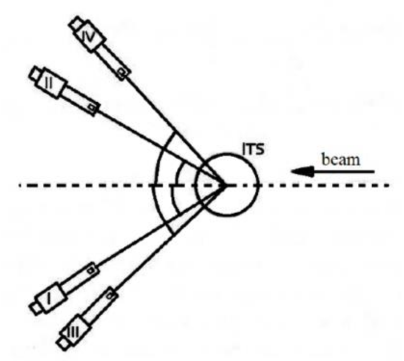

Fig.13: The view of the detector positions relative to the beam direction.

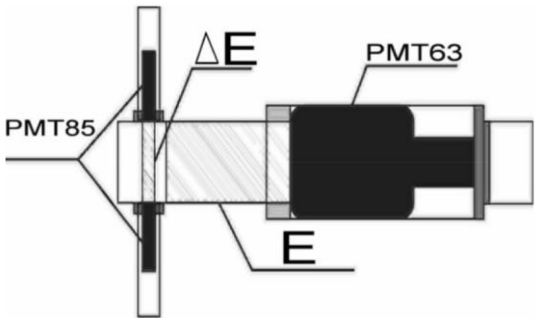

Fig.14: Schematic view of ΔE – E detector

- Protons in coincidences using ΔE – E detectors;
- Data collection for CH_2 and C targets, LED;
- Calibration measurement at 300, 400, 500 MeV;

E_d, MeV	Θ_1°	Θ_2°	E_1, MeV	E_2, MeV
300	43.5	43.5	73.9	73.9
400	43.3	43.3	98.9	98.9
500	43.0	43.0	123.9	123.9

Tab.1: Kinematic configurations for pp-quasi elastic reaction for three deuteron energies (E_d). θ_1° and θ_2° are the polar scattering angles; E_1 and E_2 are the scattered particle energies.

- Physical measurement at 300 MeV.

Configuration No.	α_1, [°]	α_2, [°]	β_1, [°]	β_2, [°]	θ_1, [°]	θ_2, [°]	ϕ_{12}, [°]
1	1.2	1.2	23.7	23.7	23.1	23.1	180
2	10.2	10.2	25.1	25.1	27	27	180
3	14	14	27.4	27.4	30.5	30.5	180
4	16.2	16.2	30.3	30.3	34	34	180
5	1.6	20.8	23.2	37.5	23.3	42.1	152.1
6	7.8	27.9	25.3	30	26.9	40.1	152.1
7	10.4	30	28.8	23	30.5	37.1	145

Tab.2: Detector location is determined by the polar and azimuthal angles. Angles α and β are the angles of mechanics.

Amplitude corrections

Using LED amplitude information

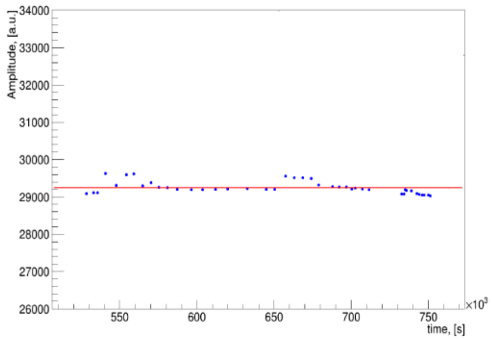

Fig.15: LED's amplitude mean value of first ΔE detector vs time for each run (blue dots).

The average amplitude value correction for each run is extracted.

Positional dependence correction of PMT's amplitude of the Δ*E* detector.

Methodical measurement:

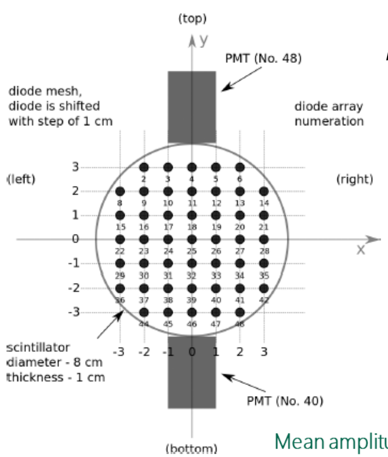

Fig.16: Setup setting: scintillator, photomultiplier tubes (No. 40, No. 48), LED positions.

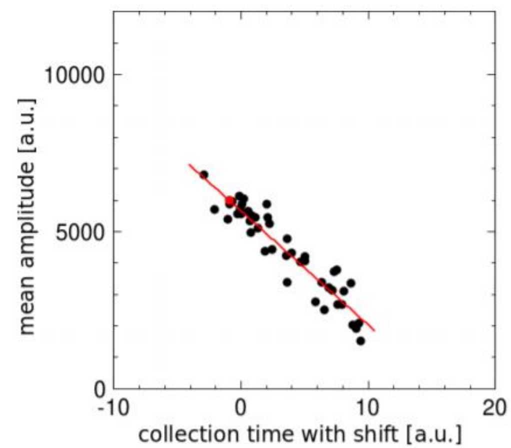

Fig.17: Mean amplitude vs collection time.

Mean amplitude: $samp = \sqrt{amp40 * amp48}$.

Red dot - amplitude value for the central geometrical point of scintillator and collected time ($stime = \sqrt{t40 * t48} - const$) value = zero.

Dependency has been fitted by straight line to obtain constant and slope values. To obtain true amplitude means to remove position amplitude dependence. The rotation about the red dot does this job.

Amplitude corrections

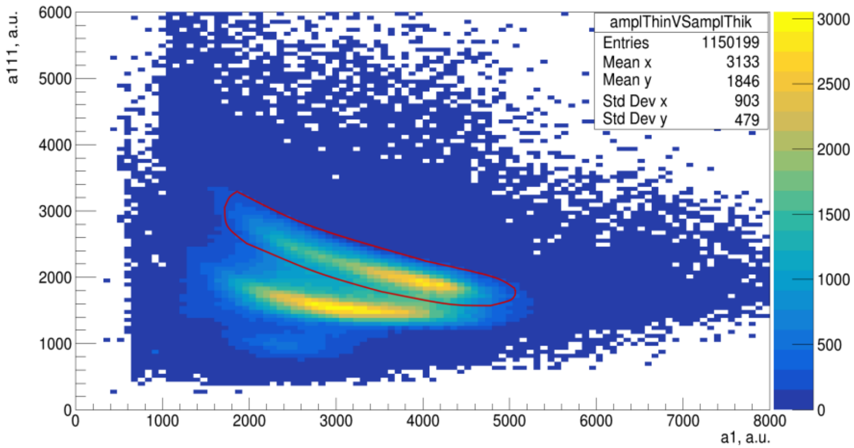

Fig.18: ΔE – E correlation.

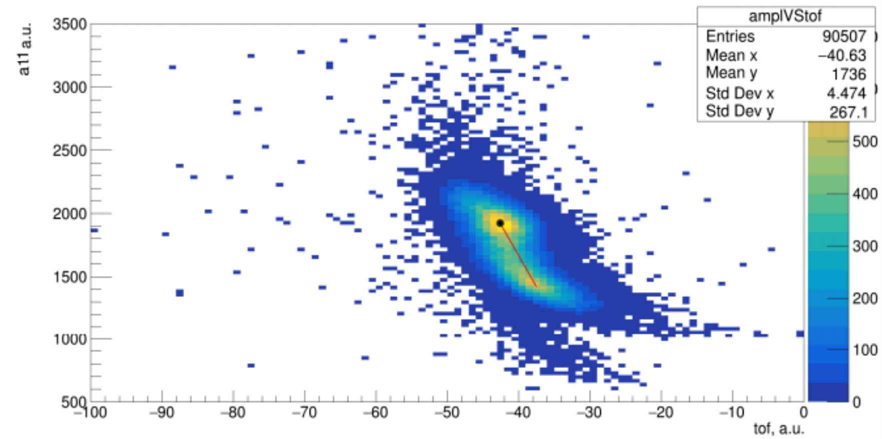

Fig.19: Samp vs. stime correlation + fit (|a1 – 4000| < 125).

$$a11_{cor} = a11 - tg\alpha * (tof_{up} - tof_{measured})$$

$a11_{cor}$ - the corrected amplitude,

α - the slope angle of the red line,

$tof_{measured}$ - the particle's time of flight - the time difference of register signal between *E* and *E* detector,

tof_{up} - the time difference of register signal between PMTs-85 positioned at thin scintillator.

Amplitude corrections

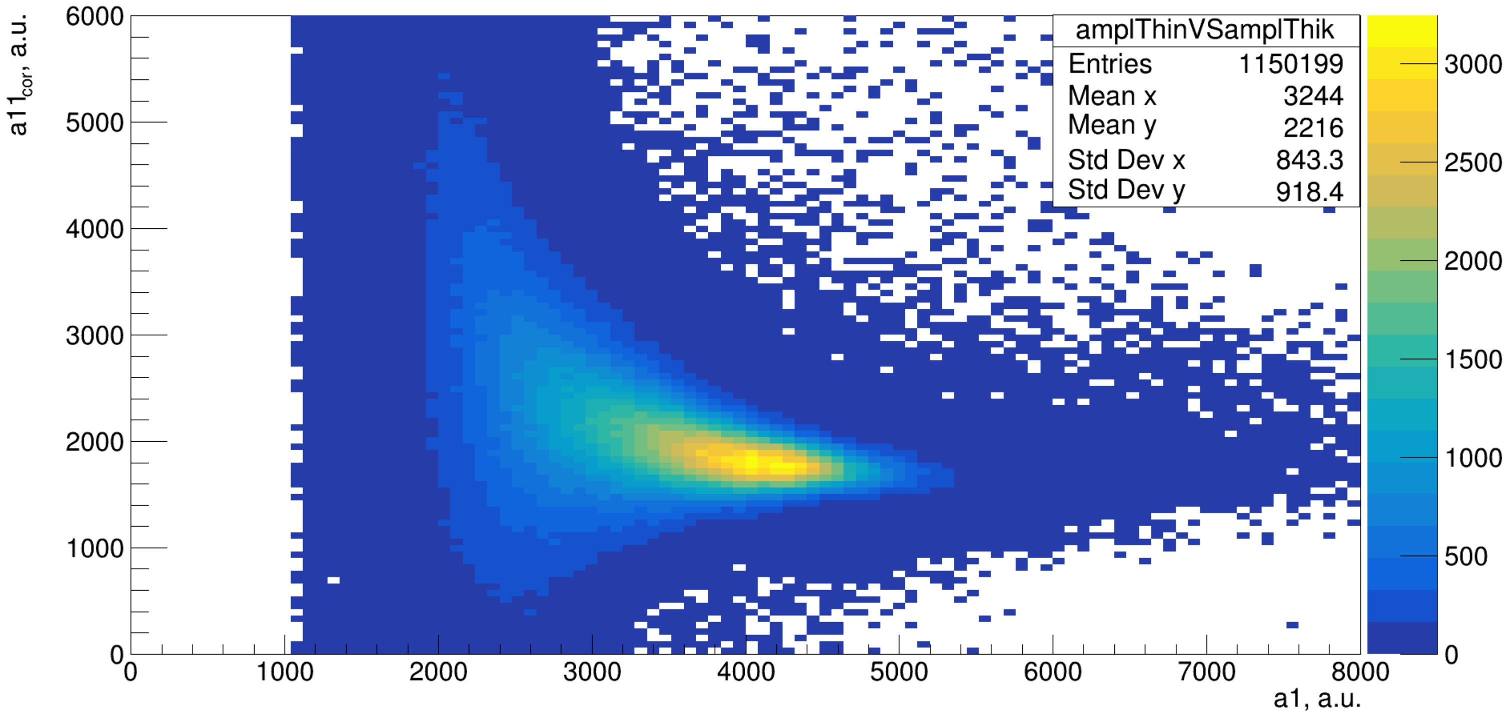

Fig.20: ΔE – E correlation with using rotation to remove position dependence.

Energy calibration

Multiplication of **the calibration coefficient** to the **amplitude** gives the information about the **energy losses** in the corresponding detector.

$$\begin{cases} k_i^1 am_i + k_i^2 A_i = 75 \\ k_i^1 am_i + k_i^2 A_i = 100 \\ k_i^1 am_i + k_i^2 A_i = 125 \end{cases}$$

The method of **least squares** →

Detector No.	k_1, a.u.	δk_1, a.u.	k_2, a.u.	δk_2, a.u.
I	0.0034	0.00017	0.028	0.002
II	0.0042	0.0002	0.028	0.003

Tab.3: The calibration coefficients (k_1 and k_2) for ΔE and E scintillators.

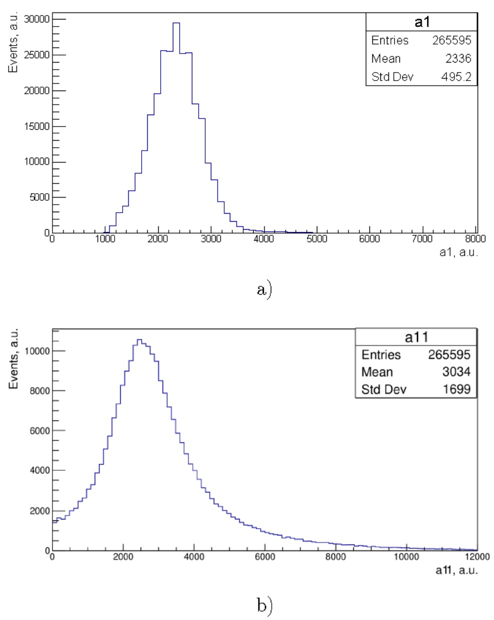

Fig. 21: Amplitude spectra for the ΔE (a) and the E (b) at the deuterons beam energy of 300 MeV.

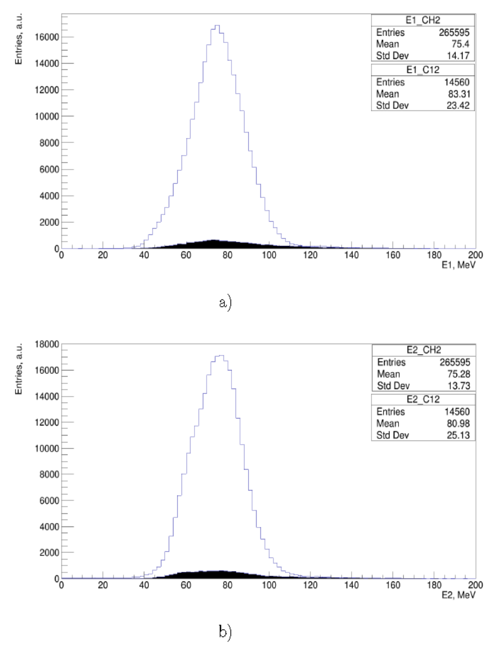

Fig. 22: The energy spectra for the first (a) and second (b) $\Delta E - E$ detectors at energy of 300 MeV.
The nonshaded histogram corresponds to CH_2 data, shaded histogram is the energy spectrum obtained on ^{12}C target

The carbon contribution is relatively small and symmetrical for the calibration measurements.

Energy calibration

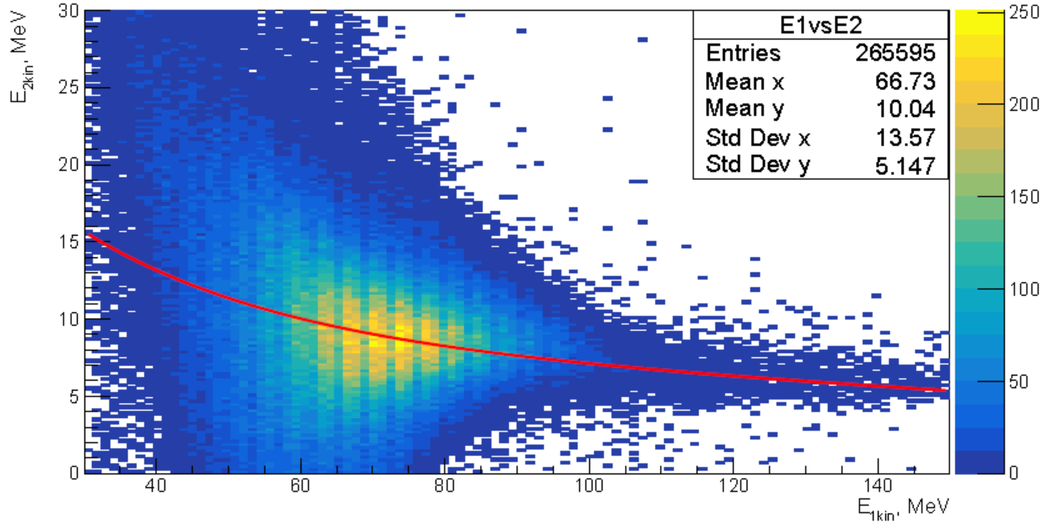

Fig. 23: Correlation of the energy losses signal in ΔE (Y-axis) and E (X-axis) detectors. The red curve represents the results of Geant4 simulation.

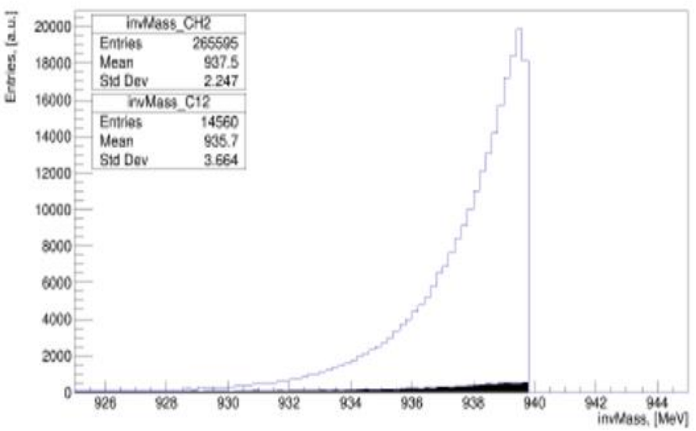

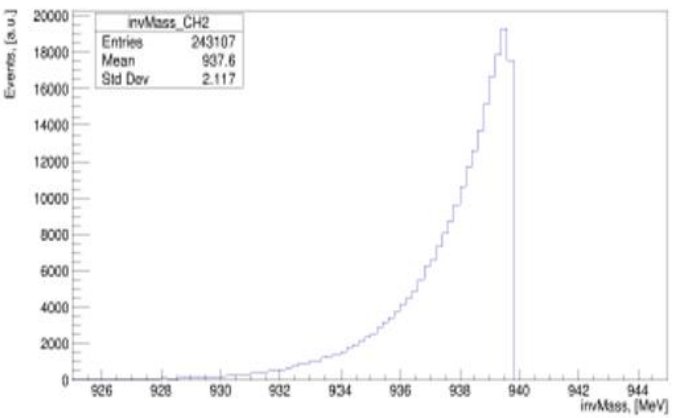

b)

Fig. 24: The missing mass spectra obtained for calibration data (a, b) and the results of TGenPhaseSpace simulation (c). Upper panel shows the missing mass spectra for CH_2 (nonshaded histogram) and ^{12}C (shaded histogram) targets. The spectrum obtained by subtracting of Carbon content from Polyethylene one is presented in b,

Detector efficiency

The detector efficiency correction needs to be applied to obtain the proper number of protons passing through the detector.

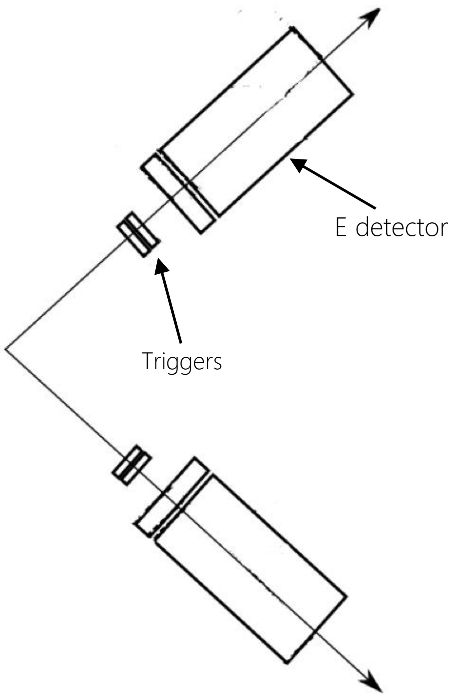

Fig.25: Detector placement for longitudinal measurements.

The various data files are used:

✓ Methodical longitudinal measurement at 43.9° (55 MeV);

$$N^{123} = \epsilon_1 \epsilon_2 \epsilon_3 N^{in},$$
$$N^{12} = \epsilon_1 \epsilon_2 N^{in},$$
$$N^{13} = \epsilon_1 \epsilon_3 N^{in},$$
$$N^{23} = \epsilon_2 \epsilon_3 N^{in},$$

ε_1, ε_2, and ε_3 - efficiency of the first, second triggers and *E* detector, respectively.

N_{123} - the number of counts detected by the three detectors in coincidence;

N_{12}, N_{13}, N_{23} - the number of events detected by two counters and detector, respectively;

N_{in} - number of "incident" events.

✓ calibration data with known mean energy of passing protons (75, 100, 125 MeV);

✓ *pp*-quasi elastic experiment at 110 ° (180 MeV).

In the case of physical measurement, where trigger counters were absent, the information from two PMTs connected to the thin scintillator taking into account.

energy, [MeV]	55	75	100	125	180
efficiency	0.407±0.0097	0.998±0.017	0.997±0.013	0.976±0.011	0.97±0.01

Tab.4: The detector efficiency for selected particles energies.

S – curve

The experimental data are projected onto the S - curve points to obtained the number of events for each point of the kinematical curve.

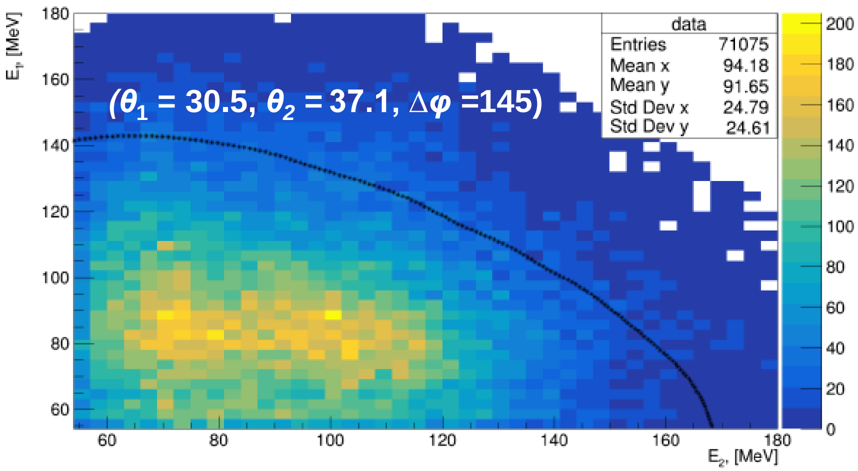

Fig.26: The correlation between the energy of the outgoing protons in the breakup. The relativistic S - curve is added as a dots with the step of 1 MeV.

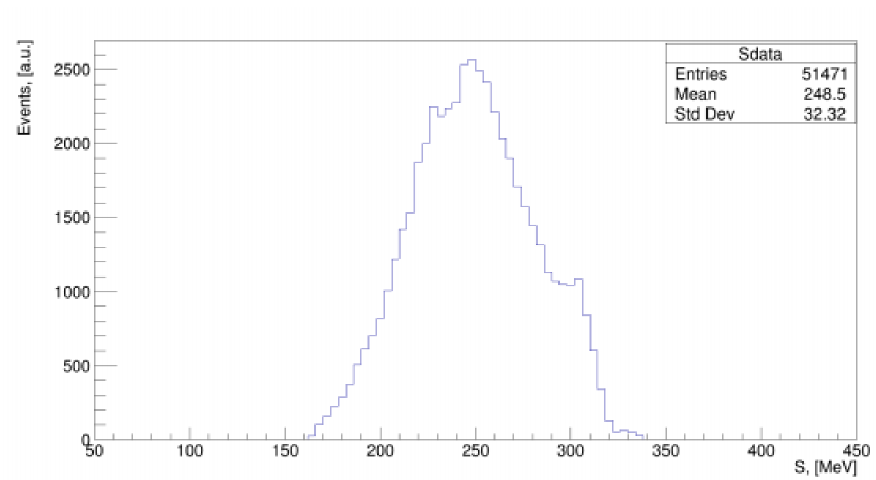

Fig.27: The results of the experimental points projection into S - curve for the data in Fig.20 within acceptance of the detector.

The number of breakup events in each point of S - curve is needed for calculation of the differential cross section in future.

Summary and conclusions

The first experiment reported in this work studies the spin observables of the dp-elastic scattering reaction at 800 MeV. The data processing consists of

- deuteron-proton **event selection** using the interaction point of the beam with the target, correlation of the energy losses in plastic scintillators for deuteron and proton and their time-of-flight difference.
- The CH2 – C procedure was performed to select the "useful" events.
- The data on the deuteron analyzing powers A_y, A_{yy} and A_{xx} at the energy of 800MeV covered the angular region of 60°–135° in the center-of-mass system were obtained at the Internal Target Station at Nuclotron. The obtained data are compared with different theoretical predictions.

The second experiment the investigation of dp-breakup reaction was performed at the kinetic energy of the deuteron beam of 300 MeV. Processing of the dp → ppn reaction can be divided into three main steps:

- The particles amplitude is corrected using information from
  – measurement with LED during data taking,
  – positional dependencies of PMT's amplitude of ΔE detector.
- The energy calibration of the ΔE – E detector has been performed at 300, 400, and 500 MeV. The calibration coefficients for ΔE and E detectors are calculated by solving the system of linear equation.
- Detector efficiencies of ΔE-E were obtained.
- Studies of the deuteron proton breakup reaction in the space star configuration were performed at 300 MeV.. Distribution of events along the kinematical S - curve has been obtained taking into account detector efficiency.

These results will be used for the calculation of the cross section of the breakup reaction.

Thank you for your attention